Fluorescent Copper(I) Complexes: Correlation of Structural and Emission Characteristics of $[\{CuI(quin)_2\}_2]$ and $[Cu_4I_4(quin)_4]$ (quin = Quinoline)†

Nigam P. Rath and Elizabeth M. Holt*
Department of Chemistry, Oklahoma State University, Stillwater, Oklahoma 74078, U.S.A.
Katsumi Tanimura
Department of Physics, Oklahoma State University, Stillwater, Oklahoma 74078, U.S.A.

Copper(I) iodide forms complexes of stoicheiometry 1:1:2 and 1:1:1 with quinoline(quin). $[\{CuI(quin)_2\}_2]$ (**1**) [monoclinic, space group $A2/a$, a = 25.620(6), b = 7.495(2), c = 20.314(4) Å, β = 111.60(1)°, Z = 8, R = 0.082 for 1 828 observed reflections] crystallizes with isolated rhombohedra of Cu_2I_2, each copper bound to the nitrogen atoms of two quinoline groups. Complex (**1**) displays a broad-band emission spectrum ($\lambda_{max.}$ 620 nm) which is independent of temperature. $[Cu_4I_4(quin)_4]$ (**2**) [triclinic, space group $P\bar{1}$, a = 12.161(8), b = 15.142(8), c = 12.162(6) Å, α = 103.75(4), β = 109.54(5), γ = 107.18(5)°, Z = 2, R = 0.095 for 2 802 observed reflections] displays a distorted parallelogram of four copper atoms, bridged on opposite edges by iodine atoms and with two additional iodine atoms face-bridging sets of three copper atoms on opposite sides of the parallelogram. The room temperature emission band ($\lambda_{max.}$ 625 nm) is broad and featureless whereas the 15-K spectrum displays considerable fine structure (490—620 nm).

Copper(I) halides form complexes with electron-pair donor ligands which display a variety of structural formats in the solid state.[1,2] Copper(I) iodide complexes have received the most attention. Common to all structural formats is the occurrence of Cu_2X_2 rhombohedra of alternating copper and halide atoms. The Cu_2X_2 rhombohedra may exist in isolation: $[\{CuI(AsPh_3)(CH_3CN)\}_2]$,[3] $[\{CuI[AsMe_2(C_6H_4NMe_2\text{-}o)]\}_2]_2]$,[4] and $[Cu_2Cl_2(PPh_3)_3]$;[5] they may share edges to form polymeric pleated sheets: $[\{CuI(py)\}_\infty]$(py = pyridine),[6] $[\{CuI(CH_3CN)\}_\infty]$,[7] $[\{CuI(2Me\text{-}py)\}_\infty]$ (2Me-py = 2-methylpyridine),[8] $[\{CuI(2,4Me_2\text{-}py)\}_\infty]$(2,4Me$_2$-py = 2,4-dimethylpyridine),[8] and $[\{CuX(PhCN)\}_\infty]$, $[\{CuX(CH_3CN)\}_\infty]$, and $[\{CuX(trans\text{-}CH_3CHCHCN)\}_\infty]$, X = Cl or Br;[9-12] two rhombs may share edges to form a chair or step structure: $[\{CuI(CH_3NC)\}_4]$,[13] $[\{CuBr(PPh_3)\}_4]\cdot 2CHCl_3$,[14] and $[\{CuCl(CH_2CHCN)\}_4]$;[15] or two rhombohedra may combine to form a cubic structure as in $[\{CuI(py)\}_4]$,[16] $[\{CuI(CH_3CN)\}_4]$·dibenzo-18-crown-6,[7]‡ $[\{Cu_2I_2(CH_3CN)(NH_2C_6H_4Cl\text{-}p)\}_2]$,[17] $[Cu_4I_4(CH_3CN)_2(NH_2C_6H_4Me\text{-}p)\}_2]$,[17] $[\{CuI(morph)\}_4]$ (morph = morpholine),[18] $[\{CuI(3Me\text{-}py)\}_4]$,[19] $[\{CuI(pip)\}_4]$ (pip = piperidine),[20] or $[\{CuI(PEt_3)\}_4]$.[21] More complicated combinations of rhombohedra have been noted in complexes of copper(I) iodide and potassium bound crown ethers§ (Cu:I ratio less than 1:1) where polymeric pleated sheets display additional bridging iodine atoms, $[K_2(15\text{-crown-}5)_2][Cu_4I_6]$, or additional edge-sharing rhombohedra bridged by additional iodine atoms, [K(dibenzo-24-crown-8)][Cu_3I_4].[22]

Complexes of CuI and a ligand may exist in more than one stoicheiometry. $[\{CuI(3Me\text{-}py)_2\}_2]$ exists as an isolated rhombohedron,[8] whereas 1:1:1 $[Cu_4I_4(3Me\text{-}py)_4]$[19] (cubic format) and 1:1:3 $[CuI(3Me\text{-}py)_3]$[2b] are also known. There are reports of 2:2:1 complexes of CuI and other methylpyridine derivatives.[23] These may have the double polymeric pleated sheet structure shown by $[\{Cu_2I_2(2Me\text{-}py)\}_\infty]$.[24]

In some instances CuI—ligand clusters of the same stoicheiometry (1:1:1) exist in more than one crystalline format. $[\{CuI(py)\}_4]$ is a cube whereas $[\{CuI(py)\}_\infty]$, is a pleated sheet polymer.[6,16] Similarly $[\{CuI(CH_3CN)\}_\infty]$, a pleated sheet, and $[\{CuI(CH_3CN)\}_4]$·dibenzo-18-crown-6, a distorted cubic structure with second sphere interactions between crown ether and acetonitrile methyl hydrogens, are both of stoicheiometry Cu:I:CH_3CN 1:1:1.[7]

These families of structures, of CuI and the same ligand, are of particular interest because the emission behaviour of the solid-state material varies with structure. $[\{CuI(py)\}_\infty]$ displays broad-band emission at room temperature and shows no shift of $\lambda_{max.}$ on cooling, whereas $[\{CuI(py)\}_4]$ displays two emission maxima corresponding to differing excitation maxima. The population of the emitting states changes with temperature. Previous correlations of structure and emission characteristics of $[Cu_4I_4(CH_3CN)_2(NH_2C_6H_4Me\text{-}p)_2]$ and $[\{Cu_2I_2(CH_3CN)(NH_2C_6H_4Cl\text{-}p)\}_2]$ suggest that Cu–Cu distances of less than 2.8 Å lead to one emission band whereas another emitting state, possibly involving metal-to-ligand charge-transfer (m.l.c.t.) behaviour or Cu–I interaction, may be responsible for a second component of the emission. Thus it is of special interest to measure emission spectra of crystalline complexes of CuI and a single ligand, which differ only in structural type and/or stoicheiometry, to identify those structural parameters which lead to the specific components of the emission spectra.

Previous references to complexes of CuI and quinoline leave some confusion about the structural identity of the emitting materials. Hardt and Gechnizdjani[25] reported the synthesis of light yellow [CuI(quin)], fluorescing orange at 20 °C (yellow-orange at −120 °C), and of yellow $[CuI(quin)_2]$, emitting orange at both temperatures. Synthesis involved stirring the

† Di-μ-iodo-bis[bis(quinoline)copper(I)] and 1,2;3,4-di-μ-iodo-1,2,4.1,2,3-di-μ_3-iodo-1,2,3,4-tetrakis(quinoline)tetracopper(I) respectively.

Supplementary data available (No. SUP 56501, 5 pp.): thermal parameters. See Instructions for Authors, *J. Chem. Soc., Dalton Trans.*, 1986, Issue 1, pp. xvii—xx. Structure factors are available from the editorial office.

‡ Dibenzo-18-crown-6 = 6,7,9,10,17,18,20,21-octahydrodibenzo[*b*,*k*]-[1,4,7,10,13,16]hexaoxacyclo-octadecin.

§ 15-Crown-5 = 1,4,7,10,13-pentaoxacyclopentadecane, dibenzo-24-crown-8 = 6,7,9,10,12,13,20,21,23,24,26,27-dodecahydrodibenz[*b*,*n*]-[1,4,7,10,13,16,19,22]octaoxacyclotetracosin.

components in acetonitrile at reduced pressures. The emission spectrum reported for the 1:1:1 complex shows a broad band of emission (r.t., $\lambda_{max.}$ *ca.* 590 nm, shoulder *ca.* 500 nm) with sharpening on cooling and a slight blue shift ($\lambda_{max.}$ 580 nm). A later published spectrum of the solid-state emission of a CuI–quin complex[26] shows broad-band room temperature (r.t.) emission ($\lambda_{max.}$ 625 nm) which develops considerable fine structure (seven recognizable maxima 490—624 nm) similar to those seen in the solution emission spectrum of quinoline alone at 77 °C but red shifted by 1 200 cm^{-1}. The structures of these specific materials were unknown. The structures of $[Cu_2I_2(quin)_4]$·quin[1] and of $[Cu_2I_2(quin)_4]$·$2CH_3CN$[27] have been reported. It is unclear whether these materials would give the emission spectra reported elsewhere.[25,26] In view of the structural variations known for complexes of CuI and ligand and in view of the opportunities these two complexes offer to correlate structural, stoicheiometric, and emission characteristics, we have determined the single-crystal *X*-ray structures of complexes of CuI–quin (1:1:1 and 1:1:2) and measured their solid-state emission spectra to allow assignment of emission characteristics to specific solid-state structural details.

Experimental

Chemicals were of Aldrich Reagent Grade and used without further purification. A freshly opened sample of quinoline was employed.

$[\{CuI(quin)_2\}_2]$ (**1**).—To an acetone (50 cm^3) suspension of CuI (0.76 g, 4 mmol) were added 5 cm^3 of a saturated aqueous solution of KI with stirring. Quinoline (1 cm^3, *ca.* 8 mmol) was added; small amounts of a light yellow precipitate were observed, and the mixture was heated under reflux for 24 h. The yellow solution was allowed to cool to room temperature; yellow prismatic crystals formed after 3 d. These crystals were observed to emit yellow when irradiated with a hand held black light (λ 254 nm) at room temperature and at liquid nitrogen temperature.

$[Cu_4I_4(quin)_4]$ (**2**).—To a 100-cm^3 suspension of CuI (1.52 g, 8 mmol) in acetone were added 15 cm^3 of a solution of saturated aqueous KI, followed by quinoline (0.5 cm^3, *ca.* 4 mmol). The mixture was heated under reflux with stirring for 24 h and crystallization allowed to proceed at 55 °C. After 3 d, the light brown diamond-shaped crystals were collected by filtration. The dry crystals were observed to emit yellow ($\lambda_{ex.}$ 254 nm) at room temperature and orange-red at liquid nitrogen temperature.

Fluorescence.—Low-temperature measurements were made with the crystals sealed in capillaries in a CTI cryogenic cooler which had a resistance heater for temperature control between 12 and 300 K. In this particular work, two detectors were used to cover the wide range of emission spectra. A cooled RCA 31034 photomultiplier tube (p.m.t.) for the visible range and an RCA 7102 p.m.t. cooled in solid CO_2 for the near-i.r. region were utilized. Emission spectra were measured on a 0.8-m Spex monochromator and excitation spectra were taken using a 0.22-m Spex monochromator. The exciting light from a 75-W Xe lamp was 'chopped' at the desired frequency. The intensity of the exciting light from the Xe lamp and a Spex Minimate monochromator was measured with a Spectra Radiometer model 301. The excitation spectra were corrected accordingly.

Single Crystal X-Ray Studies.—Crystals of $[\{CuI(quin)_2\}_2]$ (**1**) and $[Cu_4I_4(quin)_4]$ (**2**) were sealed in capillaries and mounted on a Syntex P3 automated diffractometer. Unit-cell dimensions were determined by least-squares refinement of the best angular positions for 15 independent reflections ($2\theta > 15°$) during normal alignment procedures. Data [4 490 points (**1**), 11 512 points (**2**)] were measured at room temperature using a variable scan rate, a θ—2θ scan width of 1.2° below K_{α_1} and 1.2° above K_{α_2} to a maximum 2θ value of 116°. Backgrounds were measured at each side of the scan limit for a combined time equal to the total scan time. The intensities of three standard reflections were remeasured after every 97 reflections; their intensities showed less than 5% variation, and corrections for decomposition were deemed insignificant. Data were corrected for Lorentz, polarization, and background effects. After removal of redundant [(**1**) and (**2**)] and space group forbidden data (**1**), 1 828 (**1**) and 2 802 (**2**) reflections were considered observed [$I > 3.0\sigma(I)$].

Crystal data for $[\{CuI(quin)_2\}_2]$ (**1**). $C_{18}H_{14}CuIN$, M = 448.8, monoclinic, space group $A2/a$, a = 25.620(6), b = 7.495(2), c = 20.314(4) Å, β = 111.60(1)°, U = 3 626.7(15) $Å^3$, $F(000)$ = 1 744, D_c = 1.644 g cm^{-3}, Z = 8, Mo-K_α radiation, λ = 0.710 69 Å, μ(Mo-K_α) = 28.89 cm^{-1}.

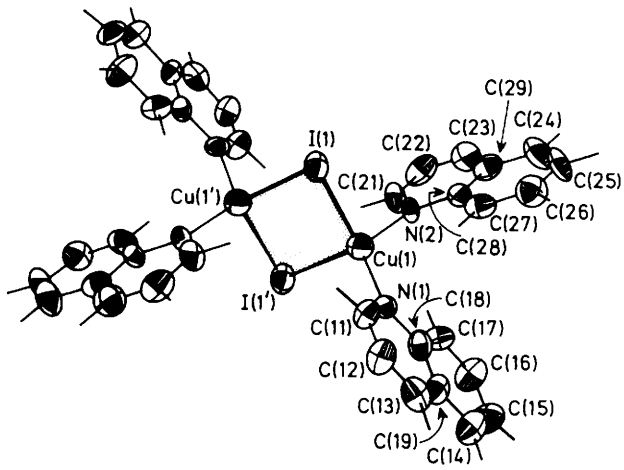

Figure 1. Projection view of $[\{CuI(quin)_2\}_2]$ (**1**)

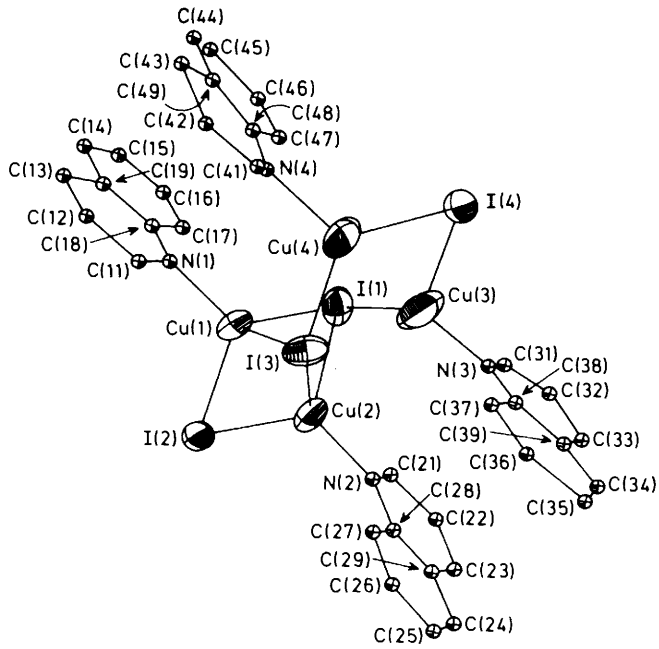

Figure 2. Projection view of $[Cu_4I_4(quin)_4]$ (**2**)

Table 1. Positional parameters for $[\{CuI(quin)_2\}_2]$ (**1**) with estimated standard deviations in parentheses

Atom	*x*	*y*	*z*
I(1)	0.959 4(1)	0.069 2(2)	0.169 6(1)
Cu(1)	1.054 0(1)	0.262 5(4)	0.221 8(2)
N(1)	1.056 1(7)	0.438 4(26)	0.145 0(9)
N(2)	1.121 0(7)	0.094 4(25)	0.271 1(9)
C(11)	1.035 6(10)	0.603 0(30)	0.140 6(13)
C(12)	1.035 6(11)	0.727 0(32)	0.090 2(15)
C(13)	1.054 8(10)	0.684 6(31)	0.040 8(13)
C(14)	1.095 8(11)	0.456 1(34)	−0.013 6(13)
C(15)	1.114 9(17)	0.291 7(62)	−0.006 8(34)
C(16)	1.118 6(12)	0.167 2(34)	0.045 6(15)
C(17)	1.098 7(10)	0.214 7(31)	0.092 6(12)
C(18)	1.077 0(9)	0.394 4(28)	0.092 4(12)
C(19)	1.076 3(9)	0.510 0(31)	0.039 8(12)
C(21)	1.110 8(9)	−0.072 8(36)	0.287 8(13)
C(22)	1.150 5(13)	−0.197 1(36)	0.324 5(15)
C(23)	1.204 1(12)	−0.146 1(38)	0.346 0(14)
C(24)	1.274 7(11)	0.087 1(44)	0.354 6(15)
C(25)	1.286 6(10)	0.250 6(42)	0.339 9(15)
C(26)	1.244 5(11)	0.368 8(35)	0.304 3(14)
C(27)	1.189 2(11)	0.315 2(32)	0.281 4(13)
C(28)	1.175 3(9)	0.143 3(29)	0.295 2(11)
C(29)	1.218 6(11)	0.023 8(35)	0.332 2(13)

Crystal data for $[Cu_4I_4(quin)_4]$ (**2**). $C_{36}H_{28}Cu_4I_4N_4$, M = 1 278.4, triclinic, space group $P\bar{1}$, a = 12.161(8), b = 15.142(8), c = 12.162(6) Å, α = 103.75(4), β = 109.54(5), γ = 107.18(5)°, U = 1 870.2(19) Å^3, $F(000)$ = 1 200, D_c = 2.270 g cm^{-3}, Z = 2, Mo-K_α radiation, λ = 0.710 69 Å, μ(Mo-K_α) = 55.52 cm^{-1}.

Solution of the structures was achieved using both direct and Patterson methods, the correctness of *E* factor maps calculated using MULTAN80[28] was assessed by checking for the appearance of suitable cross vectors in a Patterson map. Refinement of scale factors and positional and anisotropic thermal parameters for all the non-hydrogen atoms was carried out to convergence.[29] Hydrogen positional parameters for (**1**) were calculated using an appropriate geometry, C–H distance of 0.97 Å, and were included in the final cycles of refinement. Hydrogen atoms were assigned fixed isotropic thermal parameters of U = 0.03 Å^2. The final cycles of refinement [function minimized, $\Sigma(|F_o| - |F_c|)^2$] led to final agreement factors of R 0.082, R' 0.0102 (**1**), and R 0.095, R' = 0.0127 (**2**) [$R = (\Sigma||F_o| - |F_c||/\Sigma|F_o|)$; $w = 1/\sigma(F_o)$]. Scattering factors were taken from Cromer and Mann.[30] Projection views of (**1**) and (**2**) are shown in Figures 1 and 2 respectively. Positional parameters are given in Tables 1 and 2, and bond distances and angles in Tables 3 and 4.

Table 2. Positional parameters for $[Cu_4I_4(quin)_4]$ (**2**) with estimated standard deviations in parentheses

Atom	*x*	*y*	*z*
I(1)	0.396 5(3)	0.401 9(2)	0.110 8(3)
I(2)	0.036 5(3)	0.249 5(3)	−0.213 0(3)
I(3)	0.209 9(3)	0.099 7(2)	−0.004 1(2)
I(4)	0.586 0(3)	0.250 2(2)	0.336 1(3)
Cu(1)	0.151 6(5)	0.277 4(4)	0.025 3(5)
Cu(2)	0.247 7(5)	0.223 2(4)	−0.125 1(5)
Cu(3)	0.500 6(10)	0.273 1(8)	0.129 2(8)
Cu(4)	0.351 0(7)	0.218 7(8)	0.227 9(7)
N(1)	0.050 5(26)	0.278 3(20)	0.124 8(27)
N(2)	0.340 5(28)	0.217 7(22)	−0.229 4(24)
N(3)	0.623 6(32)	0.300 4(34)	0.047 5(35)
N(4)	0.226 1(43)	0.187 7(24)	0.323 0(35)
C(11)	−0.031 2(26)	0.187 1(20)	0.106 9(27)
C(12)	−0.113 1(40)	0.170 2(30)	0.169 5(41)
C(13)	−0.121 6(38)	0.257 1(27)	0.245 4(36)
C(14)	−0.032 5(34)	0.430 5(25)	0.335 5(35)
C(15)	0.057 5(47)	0.533 4(32)	0.348 5(36)
C(16)	0.135 8(45)	0.542 1(28)	0.290 6(46)
C(17)	0.137 7(38)	0.456 8(23)	0.214 6(33)
C(18)	0.053 3(32)	0.366 9(24)	0.196 3(31)
C(19)	−0.025 7(36)	0.360 6(29)	0.259 6(31)
C(21)	0.411 5(63)	0.307 5(71)	−0.219 2(52)
C(22)	0.488 9(38)	0.311 0(24)	−0.292 3(32)
C(23)	0.472 2(33)	0.220 9(34)	−0.380 8(33)
C(24)	0.373 2(29)	0.032 4(21)	−0.469 3(27)
C(25)	0.304 1(49)	−0.040 5(33)	−0.481 7(47)
C(26)	0.242 4(40)	−0.046 6(28)	−0.405 2(34)
C(27)	0.257 9(37)	0.042 2(35)	−0.321 5(33)
C(28)	0.330 7(41)	0.130 9(26)	−0.318 7(33)
C(29)	0.391 5(34)	0.136 7(26)	−0.386 6(30)
C(31)	0.702 2(30)	0.397 3(22)	0.062 0(30)
C(32)	0.797 5(38)	0.424 3(24)	0.024 0(46)
C(33)	0.801 2(45)	0.333 9(33)	−0.062 5(36)
C(34)	0.727 2(38)	0.163 8(25)	−0.151 8(39)
C(35)	0.638 0(44)	0.048 8(45)	−0.180 8(54)
C(36)	0.562 1(71)	0.075 8(64)	−0.113 7(69)
C(37)	0.543 5(51)	0.143 0(71)	−0.033 1(62)
C(38)	0.637 5(42)	0.241 6(35)	−0.016 7(37)
C(39)	0.717 8(39)	0.245 2(41)	−0.079 7(32)
C(41)	0.184 4(71)	0.114 7(49)	0.312 7(53)
C(42)	0.098 6(52)	0.080 9(72)	0.363 9(81)
C(43)	0.098 1(61)	0.156 9(57)	0.473 9(67)
C(44)	0.189 7(56)	0.351 6(37)	0.569 9(37)
C(45)	0.240 8(44)	0.425 0(27)	0.571 9(43)
C(46)	0.324 1(44)	0.450 5(31)	0.500 9(39)
C(47)	0.323 7(45)	0.370 8(43)	0.418 3(38)
C(48)	0.243 7(38)	0.276 4(42)	0.405 1(37)
C(49)	0.181 8(35)	0.262 6(23)	0.478 5(32)

Discussion

$[\{CuI(quin)_2\}_2]$ (**1**) exists in the solid state as an isolated rhombohedron of alternating copper and iodine atoms [Cu–I av. 2.686(4) Å], distorted such that the Cu atoms are in closer proximity [Cu(1)–Cu(1′), 3.364(5) Å; I(1)–Cu(1)–I(1′), 102.4(1)°] while the iodine atoms are more widely separated [I(1)–I(1′), 4.188(2) Å; Cu(1)–I(1)–Cu(1′), 77.6(1)°] than the diagonal distance (3.779 Å) of a square of side 2.686(4) Å. The Cu_2I_2 rhombohedron is planar and centred about a $\bar{1}$ symmetry element. Each copper atom is further co-ordinated to two nitrogen atoms (Cu–N av. 2.065 Å) and is of distorted tetrahedral geometry.

Direct comparisons may be drawn with similar $Cu_2I_2(quin)_4$ rhombs, with included quinoline[1] and acetonitrile molecules,[29] which display a similar planarity of the rhombohedron. $[Cu_2I_2(quin)_4]$·quin however displays a much closer Cu–Cu distance [2.866(3) Å], greater I–I separation [4.487(4) Å], and accompanying variations in I–Cu–I [114.87(5)°] and Cu–I–Cu [65.14(2)°] angles. Thus inclusion of a quinoline molecule of crystallization in the unit cell has had a significant effect on the geometry of the Cu_2I_2 rhomb. The differences must be attributed to packing influences, permitting intercalating solvent molecules to reside in planes parallel to the planes of the co-ordinated quinoline molecules, the stacking of the aromatic ring systems continuing throughout the cell. The packing of (**1**) shows no such ordering of aromatic rings (Figure 3).

The Cu–Cu separation in (**1**) is greater than that observed in the other known structural examples of isolated (non-solvated) planar Cu_2X_2 rhombohedra: $[\{CuI[AsMe_2(C_6H_4NMe_2\text{-}o)]\}_2]$ 2.73 Å,[2] $[\{CuI(AsPh_3)(CH_3CN)\}_2]$ 2.779(1) Å,[3] and $[\{CuBr(2Me\text{-}py)_2\}_2]$ 3.3491(6) Å,[31] and in the non-planar $Cu_2X_2L_3$ rhombohedron $[Cu_2Cl_2(PPh_3)_3]$ [2.909(2) Å][5] which

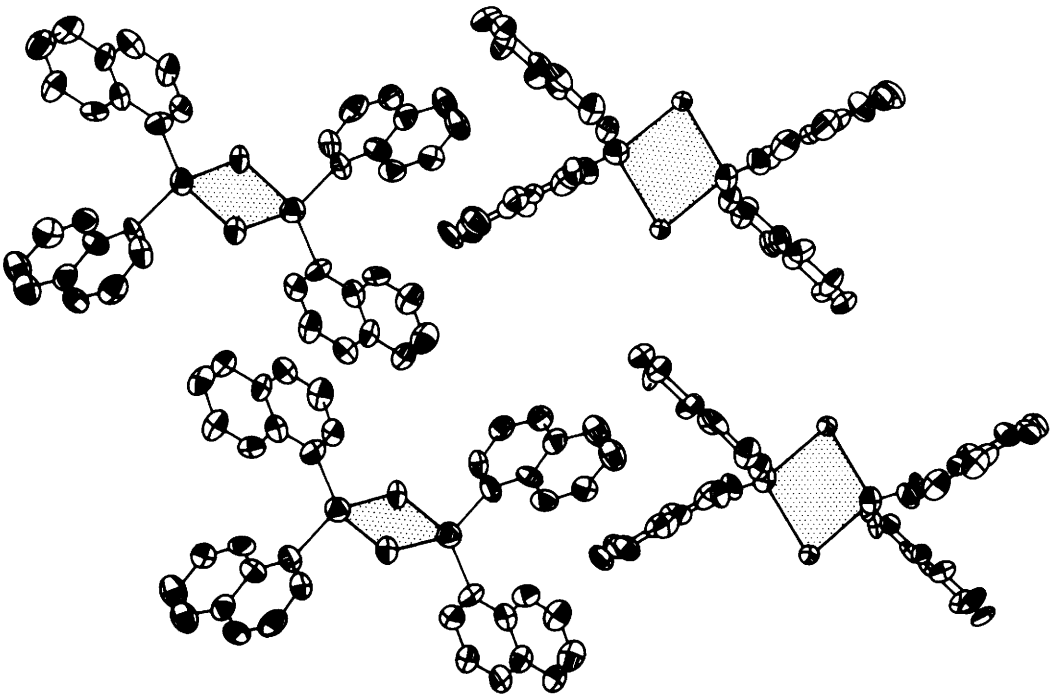

Figure 3. Packing of $[\{CuI(quin)_2\}_2]$ (**1**) in the crystal

Table 3. Bond angles (°) and distances (Å) for $[\{CuI(quin)_2\}_2]$ (**1**)*

Cu(1)–I(1)	2.685(3)	C(15)–C(16)	1.39(7)
Cu(1)–I(1′)	2.687(4)	C(16)–C(17)	1.29(4)
Cu(1)–Cu(1′)	3.364(5)	C(17)–C(18)	1.46(3)
I(1)–I(1′)	4.188(2)	N(2)–C(21)	1.35(3)
Cu(1)–N(1)	2.06(2)	N(2)–C(28)	1.34(3)
Cu(1)–N(2)	2.07(2)	C(21)–C(22)	1.38(4)
N(1)–C(11)	1.33(3)	C(22)–C(23)	1.33(4)
N(1)–C(18)	1.40(3)	C(23)–C(29)	1.38(4)
C(11)–C(12)	1.38(4)	C(29)–C(28)	1.41(3)
C(12)–C(13)	1.31(4)	C(29)–C(24)	1.42(4)
C(13)–C(19)	1.42(3)	C(24)–C(25)	1.32(5)
C(19)–C(18)	1.37(3)	C(25)–C(26)	1.38(4)
C(19)–C(14)	1.41(4)	C(26)–C(27)	1.38(4)
C(14)–C(15)	1.31(5)	C(27)–C(28)	1.39(3)
I(1)–Cu(1)–I(1′)	102.4(1)	C(17)–C(18)–C(19)	119(2)
Cu(1)–I(1)–Cu(1′)	77.6(1)	C(17)–C(18)–N(1)	118(2)
I(1)–Cu(1)–N(1)	108.2(4)	C(19)–C(18)–N(1)	123(2)
I(1)–Cu(1)–N(2)	109.4(5)	Cu(1)–N(2)–C(21)	119(1)
I(1′)–Cu(1)–N(1)	111.9(6)	Cu(1)–N(2)–C(28)	125(1)
I(1′)–Cu(1)–N(2)	102.8(6)	C(21)–N(2)–C(28)	116(2)
N(1)–Cu(1)–N(2)	120.6(8)	N(2)–C(21)–C(22)	126(2)
Cu(1)–N(1)–C(11)	122(2)	C(21)–C(22)–C(23)	117(2)
Cu(1)–N(1)–C(18)	123(1)	C(22)–C(23)–C(29)	121(2)
C(11)–N(1)–C(18)	115(2)	C(23)–C(29)–C(28)	118(2)
N(1)–C(11)–C(12)	124(3)	C(23)–C(29)–C(24)	124(2)
C(11)–C(12)–C(13)	120(2)	C(24)–C(29)–C(28)	118(2)
C(12)–C(13)–C(19)	119(2)	C(29)–C(24)–C(25)	122(2)
C(13)–C(19)–C(18)	118(2)	C(24)–C(25)–C(26)	121(2)
C(13)–C(19)–C(14)	122(2)	C(25)–C(26)–C(27)	120(2)
C(14)–C(19)–C(18)	121(2)	C(26)–C(27)–C(28)	120(2)
C(19)–C(14)–C(15)	114(4)	C(27)–C(28)–C(29)	119(2)
C(14)–C(15)–C(16)	129(6)	C(27)–C(28)–N(2)	119(2)
C(15)–C(16)–C(17)	117(3)	C(29)–C(28)–N(2)	122(2)
C(16)–C(17)–C(18)	120(2)		

* Primed atoms are related to unprimed ones by the transformation $2-x,\frac{1}{2}-y,\frac{1}{2}-z$.

is bent about the Cl–Cl axis to accommodate the geometric requirements of one tetrahedral and one trigonal-planar copper atom {*cf.* Cu–Cu in $[Cu_2Cl_2(PPh_3)_3]\cdot C_6H_6$,[32] 3.14 Å}. The difference in ring conformation and thus Cu–Cu distances in this group may be attributed to differences in the space-filling requirements of the ligands attached to copper. The bidentate (*o*-dimethylaminophenyl)dimethylarsine group occupies two co-ordination sites on a single copper atom and the constraint of its 'bite' decreases the As–Cu–N angle, opens the I–Cu–I angle, and brings the Cu–Cu atoms into closer proximity. At the other end of the series, the bulky quinoline groups of (**1**) open the N–Cu–N angle, causing the closing of the I–Cu–I angle and the greater separation of the Cu atoms across the rhombohedron.

$[Cu_4I_4(quin)_4]$ (**2**) displays a structure previously unobserved for CuI–ligand clusters; a parallelogram of copper atoms with two short sides [Cu(1)–Cu(2), 2.582(10); Cu(3)–Cu(4), 2.545(15) Å] and two long sides [Cu(2)–Cu(3), 3.279(10); Cu(1)–Cu(4), 3.325(12) Å] is bridged by four iodide atoms. The short sides of the parallelogram display μ-bridging iodide atoms [I(4) bridges Cu(3) and Cu(4); I(2) bridges Cu(1) and Cu(2)] whereas the long sides are bridged by μ_3-iodide atoms. There is a similarity of this structure to that of $[\{(CuI)_2(Ph_2PCH_2PPh_2)\}_2]$ which displays a parallelogram of four Cu atoms (short side, 2.682; long side, 3.108 Å), the short sides being bridged by μ-iodide atoms and the long sides being bridged both by μ_3-iodide atoms and by bidentate $Ph_2PCH_2PPh_2$ groups.[33] However the pattern of μ_3 binding in complex (**2**) shows the atoms of the close copper pair, Cu(1)–Cu(2), each bound to three iodide atoms whereas the atoms of the other close pair, Cu(3)–Cu(4), are each bound to two iodide atoms. In $[\{(CuI)_2(Ph_2PCH_2PPh_2)\}_2]$,[33] one member of each copper close pair is bound to two iodine atoms and the other member is bound to three iodine atoms. Each copper atom in (**2**) is bound to the nitrogen of one quinoline group. The angles about Cu(3) and Cu(4) show them to be trigonal planar in co-ordination [105.0(8)—120.8(4)°, average 114.6°] whereas Cu(2) and Cu(1) are of distorted octahedral geometry (average angle 109.6°).

Table 4. Bond angles (°) and distances (Å) for $[Cu_4I_4(quin)_4]$ (**2**)

I(1)–Cu(1)	2.680(6)	Cu(1)–Cu(4)	3.325(12)	C(13)–C(19)	1.58(6)	C(32)–C(33)	1.54(7)
I(1)–Cu(2)	2.961(6)	Cu(1)–N(1)	1.99(4)	C(14)–C(15)	1.55(6)	C(33)–C(39)	1.34(7)
I(1)–Cu(3)	2.634(14)	Cu(2)–Cu(3)	3.279(10)	C(14)–C(19)	1.27(6)	C(34)–C(35)	1.63(7)
I(1)–Cu(4)	3.394(12)	Cu(2)–N(2)	1.96(4)	C(15)–C(16)	1.36(8)	C(34)–C(39)	1.39(7)
I(1)–I(2)	4.263(5)	Cu(3)–Cu(4)	2.545(15)	C(16)–C(17)	1.41(6)	C(35)–C(36)	1.50(12)
I(1)–I(3)	4.092(5)	Cu(3)–N(3)	2.05(5)	C(17)–C(18)	1.35(5)	C(36)–C(37)	1.36(13)
I(2)–I(3)	4.245(6)	Cu(4)–N(4)	2.21(5)	C(18)–C(19)	1.41(6)	C(37)–C(38)	1.51(9)
I(2)–I(1)	4.263(5)	N(1)–C(11)	1.36(4)	C(21)–C(22)	1.49(9)	C(38)–C(39)	1.42(7)
I(2)–Cu(1)	2.624(6)	N(1)–C(18)	1.40(5)	C(22)–C(23)	1.43(6)	C(41)–C(42)	1.42(12)
I(2)–Cu(2)	2.619(8)	N(2)–C(21)	1.33(9)	C(23)–C(29)	1.33(6)	C(42)–C(43)	1.55(12)
I(3)–Cu(1)	2.951(8)	N(2)–C(28)	1.44(5)	C(24)–C(25)	1.11(6)	C(43)–C(49)	1.60(8)
I(3)–Cu(2)	2.670(7)	N(3)–C(31)	1.42(5)	C(24)–C(29)	1.56(5)	C(44)–C(45)	1.10(7)
I(3)–Cu(3)	3.268(10)	N(3)–C(38)	1.13(7)	C(25)–C(26)	1.38(8)	C(44)–C(49)	1.48(7)
I(3)–Cu(4)	2.582(7)	N(4)–C(41)	1.03(8)	C(26)–C(27)	1.40(6)	C(45)–C(46)	1.56(8)
I(4)–Cu(3)	2.531(11)	N(4)–C(48)	1.38(6)	C(27)–C(28)	1.36(6)	C(46)–C(47)	1.37(8)
I(4)–Cu(4)	2.551(9)	C(11)–C(12)	1.44(7)	C(28)–C(29)	1.28(7)	C(47)–C(48)	1.41(8)
Cu(1)–Cu(2)	2.582(10)	C(12)–C(13)	1.47(7)	C(31)–C(32)	1.38(7)	C(48)–C(49)	1.36(7)

Cu(1)–I(1)–Cu(2)	54.2(2)	Cu(2)–N(2)–C(28)	128(3)	C(27)–C(28)–C(29)	122(4)
Cu(1)–I(1)–Cu(3)	98.6(3)	C(21)–N(2)–C(28)	119(5)	C(23)–C(29)–C(24)	122(4)
Cu(2)–I(1)–Cu(3)	71.5(2)	Cu(3)–N(3)–C(31)	124(5)	C(23)–C(29)–C(28)	125(4)
Cu(1)–I(2)–Cu(2)	59.0(2)	Cu(3)–N(3)–C(38)	125(4)	C(24)–C(29)–C(28)	113(3)
Cu(1)–I(3)–Cu(2)	54.4(2)	C(31)–N(3)–C(38)	110(5)	N(3)–C(31)–C(32)	129(4)
Cu(1)–I(3)–Cu(4)	73.5(3)	Cu(4)–N(4)–C(41)	116(6)	C(31)–C(32)–C(33)	112(3)
Cu(2)–I(3)–Cu(4)	101.7(3)	Cu(4)–N(4)–C(48)	109(3)	C(32)–C(33)–C(39)	115(5)
Cu(3)–I(4)–Cu(4)	49.9(3)	C(41)–N(4)–C(48)	133(7)	C(35)–C(34)–C(39)	122(5)
I(1)–Cu(1)–I(2)	106.9(3)	N(1)–C(11)–C(12)	124(3)	C(34)–C(35)–C(36)	95(5)
I(1)–Cu(1)–I(3)	93.1(2)	C(11)–C(12)–C(13)	118(3)	C(35)–C(36)–C(37)	152(7)
I(2)–Cu(1)–I(3)	99.0(2)	C(12)–C(13)–C(19)	114(4)	C(36)–C(37)–C(38)	103(6)
I(1)–Cu(1)–N(1)	124.5(6)	C(15)–C(14)–C(19)	110(4)	N(3)–C(38)–C(37)	106(5)
I(2)–Cu(1)–N(1)	117.7(8)	C(14)–C(15)–C(16)	122(4)	N(3)–C(38)–C(39)	134(5)
I(3)–Cu(1)–N(1)	109.6(10)	C(15)–C(16)–C(17)	121(4)	C(37)–C(38)–C(39)	120(5)
I(1)–Cu(2)–I(2)	99.4(2)	C(16)–C(17)–C(18)	117(4)	C(33)–C(39)–C(34)	114(5)
I(1)–Cu(2)–I(3)	93.0(2)	N(1)–C(18)–C(17)	121(4)	C(33)–C(39)–C(38)	119(5)
I(2)–Cu(2)–I(3)	106.7(2)	N(1)–C(18)–C(19)	118(3)	C(34)–C(39)–C(38)	126(5)
I(1)–Cu(2)–N(2)	111.4(6)	C(13)–C(19)–C(14)	109(4)	N(4)–C(41)–C(42)	124(9)
I(2)–Cu(2)–N(2)	117.3(9)	C(13)–C(19)–C(18)	122(3)	C(41)–C(42)–C(43)	119(7)
I(3)–Cu(2)–N(2)	123.6(10)	C(14)–C(19)–C(18)	129(4)	C(42)–C(43)–C(49)	104(6)
I(1)–Cu(3)–I(4)	119.9(4)	C(17)–C(18)–C(19)	120(4)	C(45)–C(44)–C(49)	118(6)
I(1)–Cu(3)–N(3)	105.0(16)	N(2)–C(21)–C(22)	116(6)	C(44)–C(45)–C(46)	127(6)
I(4)–Cu(3)–N(3)	116.4(13)	C(21)–C(22)–C(23)	120(4)	C(45)–C(46)–C(47)	116(4)
I(3)–Cu(4)–I(4)	120.8(4)	C(22)–C(23)–C(29)	116(4)	C(46)–C(47)–C(48)	115(5)
I(3)–Cu(4)–N(4)	105.0(8)	C(25)–C(24)–C(29)	125(4)	N(4)–C(48)–C(47)	124(5)
I(4)–Cu(4)–N(4)	120.4(11)	C(24)–C(25)–C(26)	121(5)	N(4)–C(48)–C(49)	112(5)
Cu(1)–N(1)–C(11)	115(2)	C(25)–C(26)–C(27)	118(4)	C(47)–C(48)–C(49)	123(5)
Cu(1)–N(1)–C(18)	122(2)	C(26)–C(27)–C(28)	120(4)	C(43)–C(49)–C(44)	116(5)
C(11)–N(1)–C(18)	122(3)	N(2)–C(28)–C(27)	115(4)	C(43)–C(49)–C(48)	125(5)
Cu(2)–N(2)–C(21)	113(4)	N(2)–C(28)–C(29)	122(3)	C(44)–C(49)–C(48)	118(4)

Thus an interesting progression is shown by the series of CuX (X = Br or I) frameworks of $[\{CuBr(PPh_3)\}_4]\cdot 2CHCl_3$,[14] (**2**), $[\{(CuI)_2(Ph_2PCH_2PPh_2)\}_2]$,[33] and $[Cu_4I_4(2Me\text{-}py)_6]$[34] as a chair of stoicheiometry Cu:X:L = 1:1:1 progresses to a chair of stoicheiometry 1:1:1.5 *via* two different intermediate 1:1:1 complexes (Figure 4).

The packing of the quinoline rings about the Cu_4I_4 framework of (**2**) shows them to lie in parallel planes separated approximately by the long Cu–Cu distances of 3.302 Å (av.). The packing of the $[Cu_4I_4(quin)_4]$ molecules of (**2**) in the cell shows this close stacking of quinoline rings continuing throughout the crystal (Figure 5).

Thus the two complexes formed by CuI and quinoline are of different stoicheiometries, *i.e.* 1:1:2 (**1**) and 1:1:1 (**2**), and of markedly different structural format. Interpretation of the solid-state emission spectra of (**1**) and (**2**) is facilitated by emphasizing several specific areas of difference between the two structures. Complex (**1**) displays long Cu–Cu distances, greater than those considered representative of possible interaction. Mehrotra and Hoffmann[35] suggest that Cu^I–Cu^I distances of 2.83 Å represent overlap populations of 0.32 (binding energy −0.417 eV) from molecular orbital calculations on tetrameric Cu_4^{4+} clusters. The identification of Cu^I–Cu^I distances of 2.8 Å or less as interactive ones is also supported by the maintenance of Cu–Cu distances closely averaging 2.82 Å despite different demands of ligand geometry in a series of Cu_8S_{12} species.[36] Complex (**1**) displays non-close packing of quinoline molecules in the unit cell. Complex (**2**) shows pairs of short Cu–Cu distances, distances much shorter than those considered to represent minimal interactions between d^{10} Cu^I atoms and of the order of Cu–Cu metal distances, 2.45 Å. The aromatic quinoline ligands of (**2**) stack in parallel fashion and in close proximity.

Solid-state emission spectra measured for the two materials show very similar room temperature behaviour, while the low-temperature spectra differ considerably. At room temperature,

both show broad-band emission [$\lambda_{max.}$ 620 (**1**), 625 nm (**2**)]. For (**1**), this emission spectrum (Figure 6) is relatively unchanged on cooling to 15 K. The spectrum of (**1**) (Cu:I:quin = 1:1:2) is similar in lack of fine structure or temperature dependence to that published for [CuI(quin)] by Hardt and Gechnizdjani[25] but different in $\lambda_{max.}$ and in the lack of a shoulder at lower wavelength. A calculation of the *X*-ray powder diffraction pattern of (**1**), based on the single-crystal cell parameters determined from diffractometer data, is not compatible with the film-based *d* spacings reported for [CuI(quin)] or [CuI-(quin)$_2$][25] (Table 5), suggesting that there may be other complexes formed by CuI and quinoline and that (**1**) is previously unknown. The calculated powder pattern of (**2**) is roughly comparable with that previously reported for [CuI(quin)].[25] The low-temperature spectrum of (**2**) (Figure 7) shows the appearance of large amounts of fine structure on the high-energy side of the broad-band emission evident at room temperature. This spectrum is consistent with that published for [CuI(quin)] prepared by an unidentified synthetic route by another group of workers.[26] The relative intensity of the band at 610 nm appears reduced in ref. 26. Both spectra display great similarity to the emission spectrum of quinoline in ethanol[26] and to the low-energy segment of the total emission spectrum of quinoline reported elsewhere.[37] The fine structure of the 15-K emission spectrum of (**2**) can thus be recognized as arising from ligand alone processes in accord with the expectations that ligand alone emissions from co-ordinated ligands should display the same fine structure as the emission of the uncoordinated ligand but slightly shifted in wavelength. The appearance of this fine structure in the emission spectra of crystalline (**2**) but not (**1**) leads to the conclusion that its appearance involves $\pi \longrightarrow \pi^*$ transitions between molecules of quinoline situated in parallel planes, close packed. The 625-nm room temperature emission (610 nm, 15 K) for (**2**) which is missing in the quinoline alone spectrum,[37] and which is of considerably less intensity in the solution spectrum[26] but which constitutes the spectrum of (**1**), may be suspected to arise from m.l.c.t. interactions as observed in the solid-state emission of [$Cu_4I_4(py)_4$] ($\lambda_{max.}$ 370 nm, assigned to $d^{10} \longrightarrow d^9\pi^*)^4$ but shifted to lower energy due to the lower energy of the quinoline extended aromatic system. Consistent with the observation of emission (550—628 nm) from systems which display close Cu–Cu interactions, (**2**) but not (**1**) should have emission in this range.[17] The presence or absence of this component of the emission spectrum cannot be verified for (**1**) or (**2**) due to the m.l.c.t. component in this area.

Thus the broad-band emission spectrum of (**1**) appears to exhibit a major contribution from m.l.c.t. interactions between Cu^I and quinoline. The room temperature spectrum of (**2**) displays contributions from the same transitions and may also exhibit emission due to a mechanism involving a metal centred interaction consistent with the close proximity of Cu^I centres in the solid-state structure. Emission from (**2**) at 15 K displays an additional set of emission bands arising from ligand alone

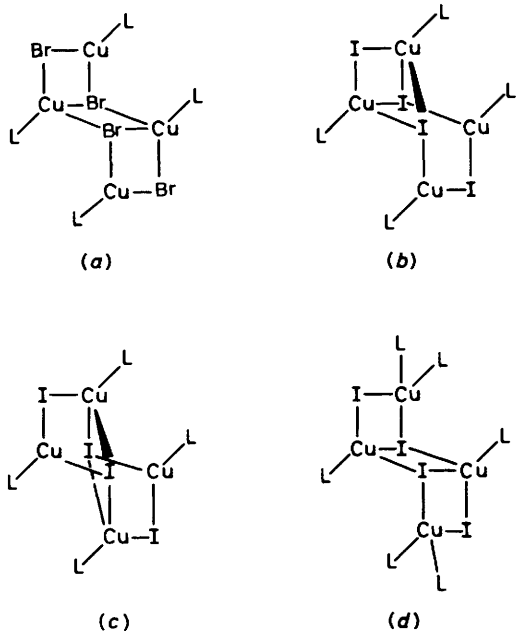

Figure 4. Comparison of CuX (X = Br or I) bonding in chair structures: (*a*) [{CuBr(PPh$_3$)}$_4$]·2CHCl$_3$,[14] (*b*) [Cu_4I_4(quin)$_4$] (**2**), (*c*) [{(CuI)$_2$(Ph$_2$PCH$_2$PPh$_2$)}$_2$],[33] and (*d*) [Cu_4I_4(2Me-py)$_6$][34]

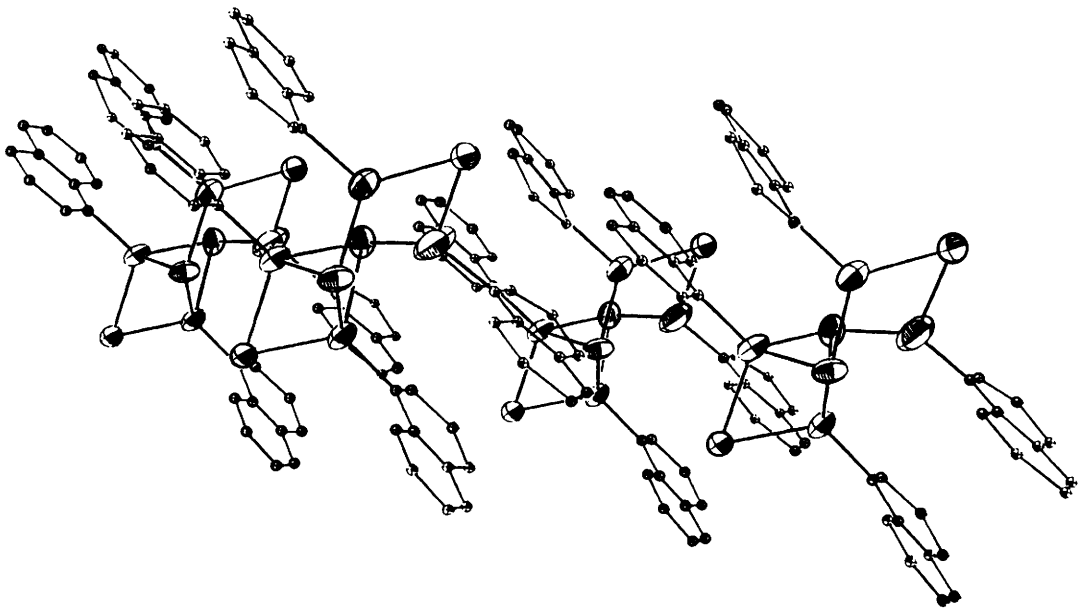

Figure 5. Packing of [Cu_4I_4(quin)$_4$] (**2**) in the crystal

Table 5. Comparison of *X*-ray powder diffraction and emission characteristics for quinoline and complexes of CuI and quinoline

Complex	λ_{max}/nm	*T*/K	λ_{max}/nm	*T*/K	Reported *d* spacings[a]	Ref.
[CuI(quin)]	590, 490 (sh)	r.t.	580, 470 (sh)	77	10.93, 10.17, 7.94, 6.93, 4.92	22
[CuI(quin)]	632	r.t.	613, 563, 540, 526, 498, 485	77	—	23
(2) $[Cu_4I_4(quin)_4]$	625	235.5	610, 565, 535, 526, 500, 490	15	*b*, 10.630, 10.622, 8.136, 7.832, 6.709, 4.963	This work
$[CuI(quin)_2]$	—	—	—	—	11.87, 9.26, 5.00	22
(1) $[\{CuI(quin)_2\}_2]$	620	251	620	15	*b*, 6.945, 6.454, 5.007, 4.916, 4.865, 4.250, 4.086, 3.670, 3.553	This work
Quinoline (EtOH glass)	—	—	552, 521, 488, 474, 461	77	—	32

[a] Those *d* spacings of greatest intensity are listed (measured from film data, Debeye camera, filtered Cu-K_α radiation). [b] Calculated from single-crystal parameters determined using Mo-K_α radiation.

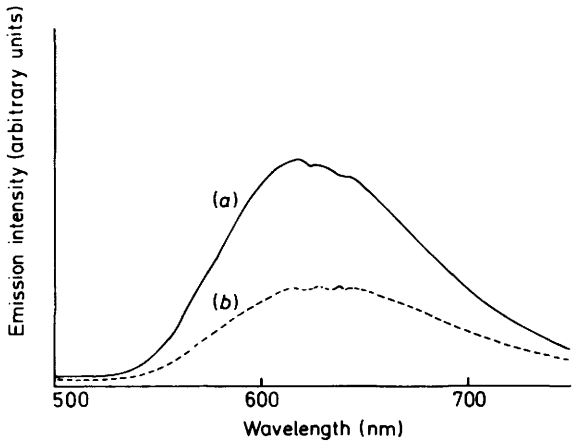

Figure 6. Emission spectra of $[\{CuI(quin)_2\}_2]$ (1) (λ_{ex} 330 nm) at (*a*) 15 and (*b*) 251 K

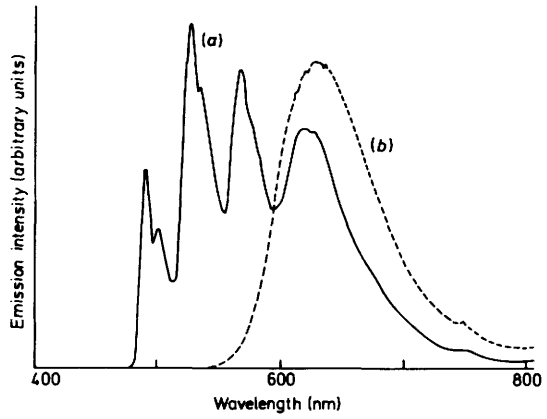

Figure 7. Emission spectra of $[Cu_4I_4(quin)_4]$ (2) (λ_{ex} 330 nm) at (*a*) 15 and (*b*) 235.5 K

interactions and suspected to arise from intermolecular quinoline interactions made possible in (2) because of the close proximity of the packed aromatic rings. The temperature dependence of the emission of (2) thus arises from a change of relative population of the collection of emitting states between room temperature and 15 K.

Acknowledgements

We thank the Petroleum Research Fund of the American Chemical Society.

References

1 P. Healy, C. Pakawatchai, and A. H. White, *J. Chem. Soc., Dalton Trans.*, 1983, 1917.
2 (*a*) J. C. Dyason, L. M. Englehardt, P. C. Healy, C. Pakawatchai, and A. H. White, *Inorg. Chem.*, 1985, **24**, 1950; (*b*) J. C. Dyason, P. C. Healy, C. Pakawatchai, V. A. Patrick, and A. H. White, *ibid.*, p. 1957.
3 M. R. Churchill and J. R. Missert, *Inorg. Chem.*, 1981, **20**, 619.
4 R. Graziani, G. Bombieri, and E. Forsellini, *J. Chem. Soc. A*, 1971, 2331.
5 V. G. Albano, P. L. Bellon, G. Ciani, and M. Manassero, *J. Chem. Soc., Dalton Trans.*, 1972, 1971.
6 E. Eitel, D. Oelkrug, W. Hiller, and J. Strahle, *Z. Naturforsch., Teil B*, 1980, **35**, 1247.
7 J. P. Jasinski, N. P. Rath, and E. M. Holt, *Inorg. Chim. Acta*, 1985, **97**, 91.
8 N. P. Rath, J. L. Maxwell, and E. M. Holt, *J. Chem. Soc., Dalton Trans.*, in the press.
9 M. Massaux and M. T. LeBihan, *Acta Crystallogr., Sect. B*, 1976, **32**, 1586, 2032.
10 M. Massaux, M. J. Bernard, and M. T. LeBihan, *Bull. Soc. Fr. Mineral. Cristallogr.*, 1969, **92**, 118.
11 M. Massaux, M. J. Bernard, and M. T. LeBihan, *Acta Crystallogr., Sect. B*, 1971, **27**, 2419.
12 M. Bolte and M. Massaux, *Inorg. Chim. Acta*, 1981, **52**, 191.
13 P. J. Fischer, N. E. Taylor, and M. J. Harding, *J. Chem. Soc.*, 1960, 2303.
14 M. R. Churchill and K. L. Kalra, *Inorg. Chem.*, 1974, **13**, 1427.
15 M. Massaux, M. T. LeBihan, and R. Chevalier, *Acta Crystallogr., Sect. B*, 1977, **33**, 2084.
16 C. L. Raston and A. H. White, *J. Chem. Soc., Dalton Trans.*, 1976, 2153.
17 N. P. Rath, E. M. Holt, and K. Tanimura, *Inorg. Chem.*, 1985, **24**, 3934.
18 V. Schramm and K. F. Fischer, *Naturwissenschaften*, 1974, **61**, 500.
19 V. Schramm, *Cryst. Struct. Commun.*, 1982, **11**, 1548.
20 V. Schramm, *Inorg. Chem.*, 1978, **17**, 714.
21 M. R. Churchill and K. L. Kalra, *Inorg. Chem.*, 1974, **13**, 1899.
22 N. P. Rath and E. M. Holt, *J. Chem. Soc., Chem. Commun.*, 1985, 665.
23 E. Eitel, Dissertation, University of Tubingen, 1979.
24 J. Strahle, W. Hiller, E. Eitel, and D. Delking, *Z. Kristallogr., Kristallgeom., Kristallphys., Kristallchem.*, 1980, **153**, 277.
25 H. D. Hardt and H. Gechnizdjani, *Z. Anorg. Allg. Chem.*, 1973, **16**, 397.
26 M. Radjaipour and D. Oelkrug, *Ber. Bunsenges. Phys. Chem.*, 1978, **82**, 159.
27 W. Hiller, *Z. Naturforsch., Teil B*, 1984, **39**, 861.
28 P. Main, S. J. Fiske, S. E. Hull, L. Lessinger, G. Germain, J. P. DeClerq, and M. M. Woolfson, MULTAN80, University of York, 1980.

29 J. M. Stewart (ed.), The *X*-RAY System – Version of 1980, Technical Report TR446, Computer Centre, University of Maryland, College Park, Maryland.
30 D. T. Cromer and I. B. Mann, *Acta Crystallogr., Sect. A*, 1968, **24**, 321.
31 V. Schramm, A. Pierre, and W. Heller, *Acta Crystallogr., Sect. C*, 1984, **40**, 1840.
32 D. F. Lewis, S. J. Lippard, and P. S. Welker, *J. Am. Chem. Soc.*, 1970, **92**, 3085.
33 N. Marsich, G. Nardin, and L. Randaccio, *J. Am. Chem. Soc.*, 1973, **95**, 4053.
34 P. C. Healy, C. Pakawatchai, C. L. Raston, B. W. Skelton, and A. H. White, *J. Chem. Soc., Dalton Trans.*, 1983, 1905.
35 P. Mehrotra and R. Hoffmann, *Inorg. Chem.*, 1978, **17**, 2187.
36 F. J. Hollander and D. Coucovanis, *J. Am. Chem. Soc.*, 1975, **96**, 5646.
37 M. A. El-Sayed, *J. Chem. Phys.*, 1963, **38**, 2834.

Received 12*th June* 1985; *Paper* 5/989